Journal of Crystal Growth 538 (2020) 125620

Contents lists available at ScienceDirect

Journal of Crystal Growth

journal homepage: www.elsevier.com/locate/jcrysgro

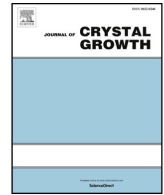

Epitaxial growth of full range of compositions of (1 1 1) $PbZr_{1-x}Ti_xO_3$ on GaN

Lin Li[a,b], Zhaoliang Liao[a,b], Minh Duc Nguyen[a], Raymond J.E. Hueting[a], Dirk J. Gravesteijn[a], Evert P. Houwman[a], Guus Rijnders[a], Gertjan Koster[a]

[a] MESA+ Institute for Nanotechnology, University of Twente, Enschede, the Netherlands
[b] National Synchrotron Radiation Laboratory, University of Science and Technology of China, Hefei 230026, Anhui, China

ARTICLE INFO

Communicated by A. Ohtomo

Keywords:
Pulsed Laser deposition
Oxides
Perovskites
Nitrides
Physical vapor deposition processes
Ferroelectric materials

ABSTRACT

Integrating functional complex oxides with conventional ("non-oxide") semiconductors emerges to be an important research field and has been attracting great interest. Because of their superior intrinsic material properties, such as a relatively high dielectric constant and polarization, the utilization of $PbZr_{1-x}Ti_xO_3$ (PZT) materials as a dielectric layer is expected to greatly improve the performance of the GaN high electron mobility transistor. The functional $PbZr_{1-x}Ti_xO_3$ exhibits quite different crystal structures and consequently physical properties depending on the composition. In this work we report the growth of full range of compositions of PZT films on MgO buffered GaN substrates. Besides revealing the temperature effect on phase formation and surface morphology, we demonstrated the strong effect of composition on the growth: pure (1 1 1) phase is formed in Ti-rich PZT ($x > 0.48$) while pyrochlore impurity phase is found in Zr-rich PZT ($x < 0.48$). By introducing an ultrathin Ti-rich PZT seed layer, we are able to achieve epitaxial growth of Zr-rich PZT. The epitaxial PZT films of different composition all exhibit good ferroelectric properties, showing great promise for future GaN device applications.

1. Introduction

The semiconductor GaN is an important material with many potential applications such as field effect transistor (FET) in high power and high frequency devices due to its direct, wide band gap of 3.45 eV at room temperature and high chemical and mechanical stability [1,2]. Furthermore, GaN-on-silicon offers many advantages such as good electrical and thermal conductivity, large size availability, mass production, and significantly low cost for GaN optoelectronic and microelectronic devices. The utilization of ferroelectric $PbZr_{1-x}Ti_xO_3$ (PZT) materials as a dielectric layer is expected to further improve the performance of GaN/AlGaN high electron mobility transistor (HEMT). The superior material properties including high permittivity, excellent ferroelectric, piezoelectric, and electromechanical properties [3] are expected to make PZT an ideal material for improving the tradeoff between the breakdown voltage and the specific on-resistance of the GaN/AlGaN HEMT as well as realizing resonators, non-volatile FETs in a GaN platform [4–7].

A lot of effort has been spent to achieve high quality PZT films on GaN [8–14]. However, the highly incompatible crystal lattice, different lattice constant, and chemical reactivity between PZT and GaN hinder the epitaxial growth of PZT [8–13]. The employment of buffer layers has been found to improve the film quality. For example, with an atomically flat ultrathin MgO buffer layer, we previously realized the epitaxial growth of highly crystalline PZT ($x = 0.48$) films with excellent ferroelectric properties, which opens the possibility to practically use advanced oxide materials in GaN HEMTs [13]. Depending on the composition the PZT possesses quite a different crystal structure and consequently physical properties [3,15]. A morphotropic phase boundary (MPB) at $\times = \sim 0.48$ separates the rhombohedral ($x < 0.48$) from tetragonal phase ($x > 0.48$). The direction of ferroelectric domains also depends on the composition. At the MPB, PZT exhibits the highest dielectric constant. The polarization direction is along the pseudocubic [0 0 1] direction in tetragonal PZT ($x > 0.48$) while it is along pseudocubic (1 1 1) direction for rhombohedral PZT ($x < 0.48$). Different compositions are suitable for different types of applications, hence it is highly desired to study the epitaxial growth of different compositions of PZT on GaN. In contrast to the growth of PZT on typical perovskite substrates such as $SrTiO_3$ and $GdScO_3$ where growth is nearly composition independent [16,17], the growth of a different composition of PZT on MgO/GaN is non-trivial. Our results demonstrate that epitaxial growth is favored when $\times > 0.48$ while

E-mail address: g.koster@utwente.nl (G. Koster).

https://doi.org/10.1016/j.jcrysgro.2020.125620
Received 15 October 2019; Received in revised form 8 March 2020; Accepted 19 March 2020
Available online 21 March 2020
0022-0248/ © 2020 The Author(s). Published by Elsevier B.V. This is an open access article under the CC BY license (http://creativecommons.org/licenses/BY/4.0/).

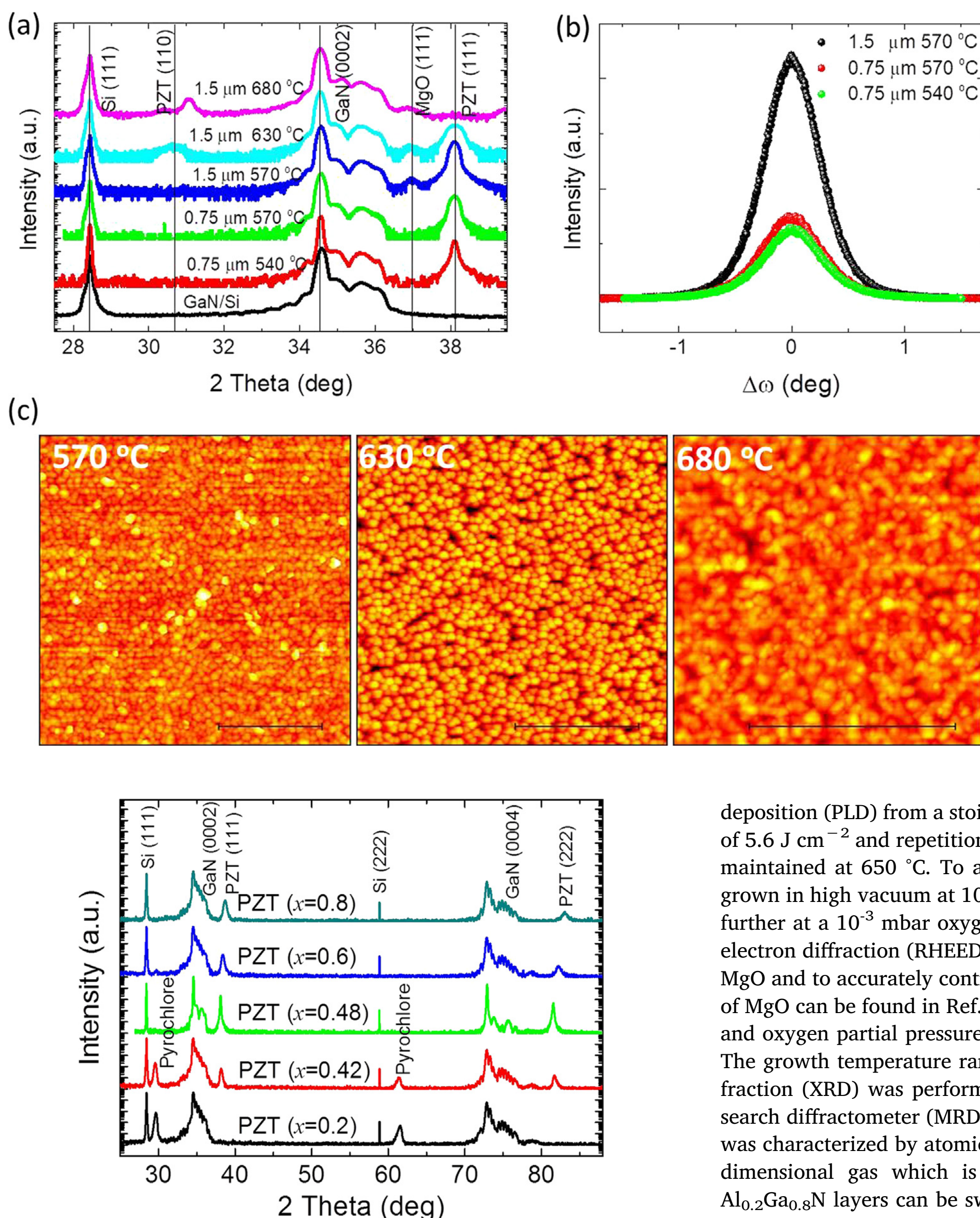

Fig. 1. XRD θ-2θ scan of PZT ($x = 0.48$) films on MgO buffered GaN/Si substrates grown at different temperatures. Data of pure GaN/Si substrate (black) is shown for comparison. (b) The rocking curves of the PZT (1 1 1) peaks for films grown at 570 °C (black and red curves) and 540 °C (green curve). (c) The surface morphology by AFM of 1.5 μm thick PZT films grown at different temperatures. The scale bar is 2 μm. The thickness of MgO buffer layer for 1.5 μm and 0.75 μm thick PZT films are 115 nm and 11 nm respectively.

Fig. 2. XRD θ-2θ scans of 750 nm PZT films with different compositions on MgO buffered GaN substrates. The thickness of MgO buffer layer is 0.5 nm.

the non-ferroelectric pyrochlore phase will form when $\times < 0.48$. By introducing PZT ($x = 0.8$) as an additional seed layer, we further realized the epitaxial growth of Zr-rich PZT ($x < 0.48$) films. In other words, we demonstrate that the complete PZT family can be epitaxially grown on MgO buffered GaN substrates. The physical properties of these (1 1 1) PZT layers on GaN are found to strongly depend on the composition, paving a path to diverse device applications.

2. Experimental

The PZT films were grown by pulsed laser deposition (PLD) on MgO buffered GaN using a ceramic PZT target. In order to compensate the loss of volatile Pb during the PLD deposition, an excess 10% Pb was added in the target [18,19]. The GaN was epitaxially grown on Si (1 1 1) substrates by metal organic chemical vapour deposition (MOCVD) with multiple $Al_{1-x}Ga_xN$ buffer layers to release the strain from Si. Detail on GaN/Si substrates can be found in Supplemental in Ref. [13]. The MgO films were grown on GaN substrates by pulsed laser deposition (PLD) from a stoichiometric MgO ceramic target at a fluence of 5.6 J cm^{-2} and repetition rate of 5 Hz. The growth temperature was maintained at 650 °C. To avoid oxidation of GaN, the MgO was first grown in high vacuum at 10^{-7} mbar for 2 min (500 pulses), then grown further at a 10^{-3} mbar oxygen partial pressure. Reflection high energy electron diffraction (RHEED) was used to monitor in-situ the growth of MgO and to accurately control its thickness. More details of the growth of MgO can be found in Ref. 13. Regarding the PZT growth, the fluence and oxygen partial pressure were 2 J/cm^2 and 0.1 mbar, respectively. The growth temperature ranged from 540 °C to 680 °C. The x-ray diffraction (XRD) was performed using PANalytical-X 'Pert materials research diffractometer (MRD) in high resolution mode. The morphology was characterized by atomic force microscopy (AFM). Given that the 2 dimensional gas which is buried underneath top insulating GaN/$Al_{0.2}Ga_{0.8}N$ layers can be switched off by up polarization of PZT layer and thus full P-E loop cannot be measured, 2 dimensional gas could not be used as bottom electrode. Instead, an in-plane capacitor configuration was used for ferroelectric measurement. The in-plane electrodes for ferroelectric measurement were fabricated with standard photo lithography, Ti and Pt sputter deposition and lift-off. The ferroelectric properties were measured using the AixAcct TF-2000 Analyzer at a frequency of 1 kHz.

3. Results

First, the effect of growth temperature on the quality of PZT ($x = 0.48$) was investigated. Fig. 1a shows the XRD scan of 1.5 μm PZT ($x = 0.48$) on 115 nm MgO buffered GaN. At a relatively high growth temperature of 680 °C, only non-epitaxial (1 0 1)/(1 1 0) phase was observed. The preferred formation of {1 1 0} phase at high temperature is presumably due to a difference in nucleation energy of (1 1 1) PZT compared to {1 1 0} PZT, apparently causing a higher temperature to favor the formation of the {1 1 0} phase [20]. When the growth temperature was decreased to 630 °C, the {1 1 0} impurity phase was suppressed and a large amount of epitaxial (1 1 1) phase was formed. The lower growth temperature also resulted in less crystallinity of (1 0 1) and (1 1 0) phase, broadening both (1 0 1) and (1 1 0) peaks.

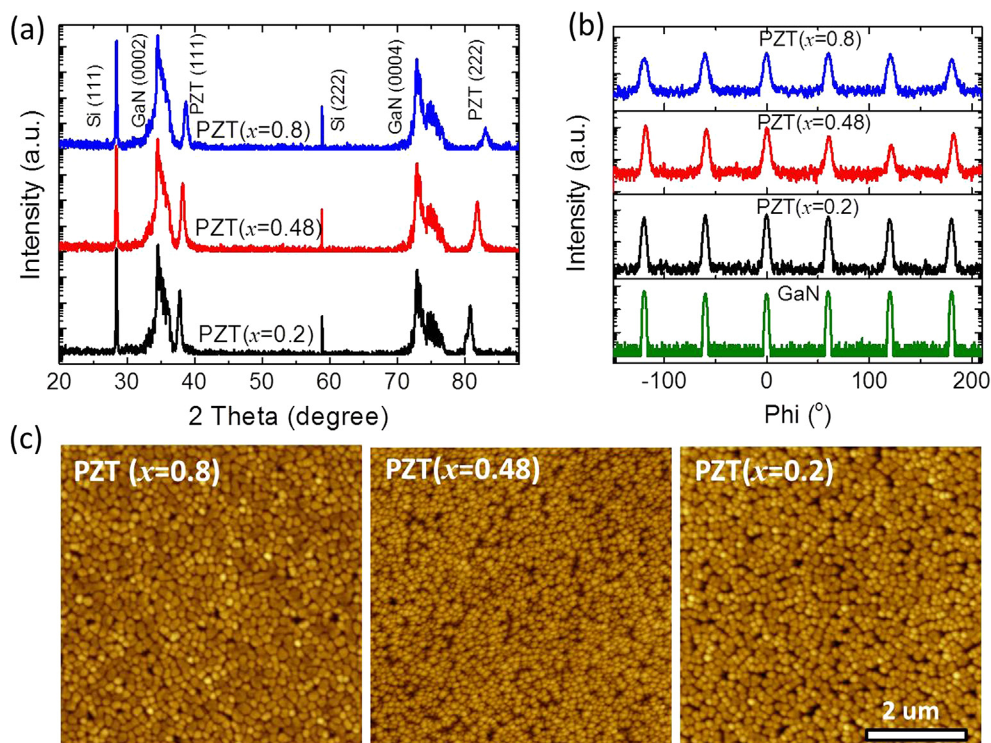

Fig. 3. (a) XRD θ-2θ scans and (b) Phi-scans of (4 2 0) peaks of 750 nm PZT(x = 0.2), PZT(x = 0.48) films on PZT(x = 0.8)/MgO/GaN (with a 5 nm PZT (x = 0.8) seed layer) and 750 nm PZT(x = 0.8) film on MgO/GaN. In (b) GaN (1–24) is shown for comparison. (c) AFM surface morphology of the PZT films.

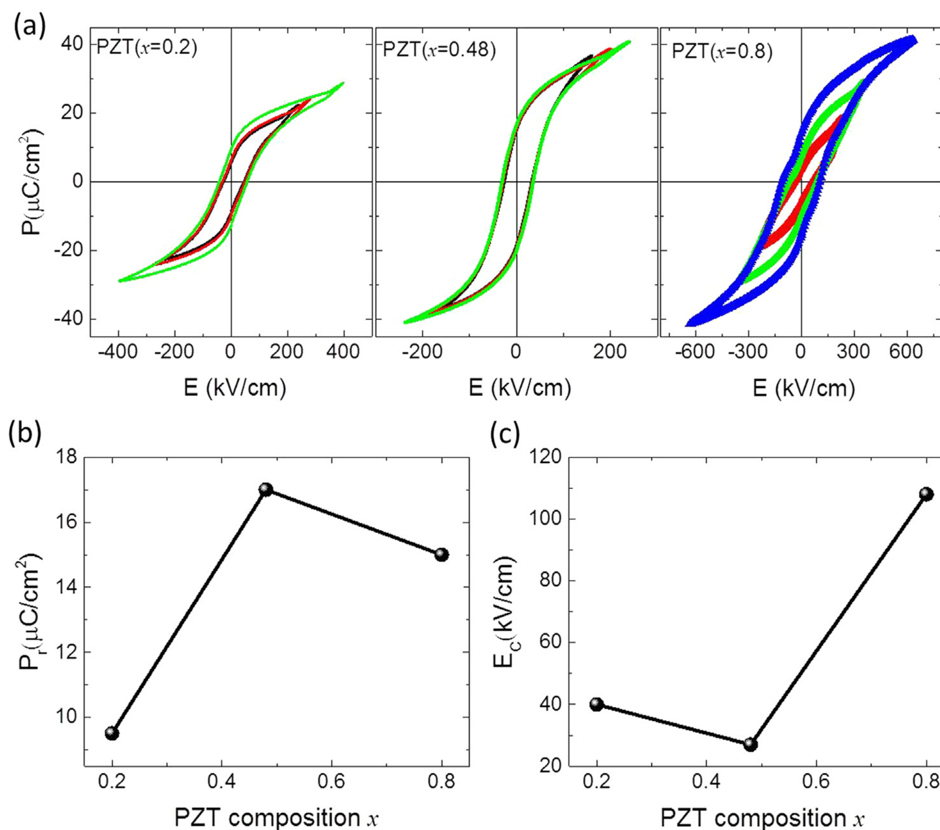

Fig. 4. (a) Measured *P-E* loops, the inset in the PZT (x = 0.2) panel shows the in-plane electrode configuration; (b) extracted remnant polarization (P_r); (c) extracted coercive field (E_C) of PZT (750 nm) films of different composition on MgO (0.5 nm)/GaN substrates. For PZT (x = 0.2) and PZT (x = 0.48) films growth, an additional 5 nm PZT (x = 0.8) seed layers were grown first on MgO/GaN.

Therefore, (1 0 1) and (1 1 0) merge to behave like single broad peak. At an even lower temperature of 570 °C, only the (1 1 1) orientation was observed. Similar to a previous report [13], the epitaxial growth of PZT was not affected by the thickness of MgO buffer layer. If reducing the MgO buffer layer thickness to 11 nm, high quality of epitaxial PZT was still obtained (see red curve in Fig. 1a). Surprisingly, single (1 1 1) orientation was still observed even at the relatively low growth temperature of 540 °C. Fig. 1b shows the rocking curve of PZT (1 1 1) peak

of different films grown at 570 °C and 540 °C. The full width at half maximum (FWHM) of 1.5 μm PZT on MgO(115 nm)/GaN, 0.75 μm PZT on MgO(11 nm)/GaN both grown at 570 °C, and 0.75 μm PZT on MgO (11 nm)/GaN grown at 540 °C is 0.59°, 0.62° and 0.61°, respectively. Therefore, lowering the growth temperature to 540 °C didn't seem to affect the film quality, making it more suitable for practical applications. For PLD growth, it is known that too low growth temperature will degrade the crystallinity. Further, previous experiment indicated that (0 0 1) orientated PZT is favored at low growth temperature which then will introduce impurity phase [20]. Therefore, 540 °C − 570 °C appears to be an optimized growth temperature. In addition, the presence of impurity phases affects the surface morphology as characterized by AFM. As shown in Fig. 1c, the pure (1 1 1) phase has a dense grain and smooth surface with a roughness Rms of 3.0 nm. The film grown at 630 °C with a mixture of (1 0 1)/(1 1 0) and (1 1 1) phases has columnar structures with a gap between the columns. The roughness of this film is 29 nm. The pure (1 0 1)/(1 1 0) phase grown at 680 °C shows a roughness of 6 nm.

Using these optimized growth conditions, PZT films with other compositions were grown as well. Fig. 2 shows the XRD θ-2θ scans of 750 nm PZT films with different compositions grown on 0.5 nm MgO buffered GaN at 570 °C. As mentioned in our previous report, the MgO on GaN is stress free and a 0.5 nm MgO buffer layer is already thick enough for the epitaxial growth of PZT [13]. It was found that there are no impurity peaks for × ≥ 0.48 films, but the × < 0.48 films exhibit the mixture of (1 1 1) PZT and pyrochlore phase. The (1 1 1) PZT phase even fully disappeared for PZT (x = 0.2). Apparently, the Zr-rich favors the formation of impurity pyrochlore phase. It is consistent with a previous report that the perovskite transformation temperature is lower in Ti-rich PZT than in Zr-rich PZT films.[21]

In order to epitaxially grow Zr-rich PZT ($x < 0.48$), a 5 nm ultrathin Ti-rich PZT ($x = 0.8$) was used as a seed layer for the growth of Zr-rich PZT. With these PZT ($x = 0.8$) seed layers, we were able to epitaxially grow all compositions of PZT on MgO buffered GaN as shown in Fig. 3a. The XRD scan shows a pure PZT (1 1 1) phase for PZT ($x = 0.2$) films. More generally, all PZT compositions including Ti-rich PZT can be grown epitaxially on MgO/GaN by introducing a PZT ($x = 0.8$) seed layer (see Fig. 3a), e.g., PZT ($x = 0.48$). To further prove the epitaxial relationship, Phi-scans of PZT (4 2 0) and GaN (−1 2 4) peaks were performed (see Fig. 3b). The PZT peaks were found to be fully aligned with GaN (−1 2 4) peaks, demonstrating the epitaxial relationship of PZT on GaN. The surface morphology of the PZT films is shown in Fig. 3c. Typical columnar structures reflected by the grain structure at the surface are densely arranged.

The ferroelectric properties of these 750 nm thick, epitaxial PZT thin films were investigated by measuring *P–E* (polarization versus electric field) loops. Since a bottom electrode was absent, the *P-E* loop was measured using an in-plane configuration as described in our previous report [13]. The *P-E* loops were measured with a ferroelectric tester (AixAcct TF-2000 Analyzer) at a frequency of 1 kHz. Characteristic hysteretic *P-E* loops were observed for all PZT films with different compositions (see Fig. 4), demonstrating the ferroelectric properties of the PZT films. The remnant polarization (P_r) extracted from the *P-E* loop for different compositions is shown in Fig. 4b. The remnant polarization of PZT ($x = 0.48$) is about 17 μC/cm^2 and is found to be larger than PZT ($x = 0.2$) and PZT ($x = 0.8$). The coercive field is found to be composition dependent as well (see Fig. 4c). The PZT ($x = 0.8$) possesses the highest coercive field of 108 kV/cm, about 4 times that of PZT ($x = 0.48$) and 2.7 times that of PZT ($x = 0.2$). The composition dependent coercive field can be explained by the introduction of different density of defect dipoles [22]. More defect dipoles are created with higher Zr/Ti disorder, e.g., at Zr/Ti ≈ 1, making the domain switching easier and therefore inducing lower coercive field [22]. Due to the large coercivity, the PZT ($x = 0.8$) requires a much higher voltage to saturate the polarization (see Fig. 4a).

4. Conclusions

In summary, the growth of PZT on MgO/GaN is found to be composition dependent. Pure epitaxial PZT (1 1 1) phase can be achieved for Ti-rich PZT which is located to the right side of the MPB. In contrast, the Zr-rich PZT which is located at the left side of the MPB is found to more easily form pyrochlore impurity phase. This composition dependent phase formation should be linked to the fact that the Ti-rich PZT has a lower perovskite transformation temperature than Zr-rich PZT [21]. The perovskite phase is more stable in Ti-rich PZT compounds. Regarding that the lattice constant of PZT which ranges from 4.0 Å to 4.1 Å depending on the composition × has relative large mismatch with MgO (2.6–5%), the introduction of PZT (x = 0.8) seed layer can relax the large strain from MgO. Additionally, the PZT seed layer can provides a perovskite surface template to guide the formation of perovskite phase. Therefore, the introduction of a Ti-rich perovskite PZT as an additional buffer layer can greatly suppress the pyrochlore phase, leading to epitaxial growth of Zr-rich PZT.

Finally, the physical properties of these (1 1 1) PZT layers on GaN strongly depend on the composition. The PZT ($x = 0.48$) located at the MBP boundary has relative larger remnant polarization and lower coercive field than the other compositions. The PZT ($x = 0.8$) is found to have the highest coercive field. The different properties of PZT with different compositions can be used for different specific applications, such as high power FET's and non-volatile memory ferroelectric controlled electronics device. Our strategy to realize epitaxial growth of PZT films with different compositions on GaN opens a new avenue for oxide-III-IV semiconductor electronics.

Declaration of Competing Interest

The authors declare that they have no known competing financial interests or personal relationships that could have appeared to influence the work reported in this paper.

Acknowledgements

Lin Li acknowledges financial support from Nano Next NL (Grant no. 7B 04). The authors acknowledge NXP for providing the GaN/AlGaN/Si (111) wafer.

References

[1] Tyler J. Flack, Bejoy N. Pushpakaran, Stephen B. Bayne, GaN Technology for Power Electronic Applications: A Review, J. Electron. Mater. 45 (2016) 2673.

[2] S.J. Pearton, F. Ren, A.P. Zhang, G. Dang, X.A. Cao, K.P. Lee, H. Cho, B.P. Gila, J.W. Johnson, C. Monier, C.R. Abernathy, J. Han, A.G. Baca, J.-I. Chyi, C.-M. Lee, T.-E. Nee, C.-C. Chuo, S.N.G. Chu, GaN electronics for high power, high temperature applications, Mater. Sci. Eng. B 82 (2001) 227.

[3] B. Jaffe, H. Jaffe, W.R. Cook, Piezoelectric ceramics, London: Academic Press.

[4] Y.S. Kang, Q. Fan, B. Xiao, Y.I. Alivov, J.Q. Xie, N. Onojima, S.-J. Cho, Y.-T. Moon, H. Lee, D. Johnstone, H. Morkoc, Y.-S. Park, Fabrication and current-voltage characterization of a ferroelectric lead zirconate titanate/ field effect transistor, Appl. Phys. Lett. 88 (2006) 123508.

[5] S.K. Dey, S. Bhaskar, M.H. Tsai, W. Cao, Pb(Zr, Ti)$_O$3-GaN Heterostructures for RF MEMS Applications, Integr. Ferroelectr. 62 (2004) 69.

[6] W.P. Li, R. Zhang, Y.G. Zhou, J. Yin, H.M. Bu, Z.Y. Luo, B. Shen, Y. Shi, R.L. Jiang, S.L. Gu, Z.G. Liu, Y.D. Zheng, Z.C. Huang, Studies of metal–ferroelectric–GaN structures, Appl. Phys. Lett. 75 (1999) 2416.

[7] I. Stolichnov, L. Malin, P. Muralt, N. Setter, Nonvolatile gate effect in the PZT/AlGaN/GaN heterostructure, J. Eur. Ceram. Soc. 27 (2007) 13.

[8] K. Elibol, M.D. Nguyen, R.J.E. Hueting, D.J. Gravesteijn, G. Koster, G. Rijnders, Integration of epitaxial $Pb(Zr_{0.52}Ti_{0.48})O_3$ films on GaN/AlGaN/GaN/Si(111) substrates using rutile TiO_2 buffer layers, Thin Solid Films 591 (2015) 66.

[9] B. Xiao, X. Gu, N. Izyumskaya, V. Avrutin, J.Q. Xie, H.Y. Liu, H. Morkoc, Structural and electrical properties of Pb(Zr, Ti)$_O$3 grown on (0001) GaN using a double PbTi$_O$3/PbO bridge layer, Appl. Phys. Lett. 91 (2007) 182908.

[10] Y.R. Li, J. Zhu, W.B. Luo, Study of the integrated growth of dielectric films on GaN semiconductor substrates, IEEE T Ultrason Ferr. 57 (2010) 2192.

[11] E.A. Paisley, H.S. Craft, M.D. Losego, H. Lu, A. Gruverman, R. Collazo, Z. Sitar, J.-P. Maria, Epitaxial $Pb_xZr_{1-x}TiO_3$ on GaN, J. Appl. Phys. 113 (2013) 074107.

[12] S.K. Dey, W. Cao, S. Bhaskar, J. Li, Highly textured $Pb(Zr_{0.3}Ti_{0.7})O_3$ thin films on

GaN/sapphire by metalorganic chemical vapor deposition, J. Mater. Res. 21 (2006) 1562.
[13] L. Li, Z.L. Liao, N. Gauquelin, M.D. Nguyen, R.J.E. Hueting, D.J. Gravesteijn, I. Lobato, E.P. Houwman, S. Lazar, J. Verbeeck, G. Koster, G. Rijnders, Epitaxial Stress-Free Growth of High Crystallinity Ferroelectric $PbZr_{0.52}Ti_{0.48}O_3$ on GaN/AlGaN/Si (111) Substrate, Adv. Mater. Inter. 5 (2017) 1700921.
[14] H. Hanawa, K. Horio, Increase in breakdown voltage of AlGaN/GaN HEMTs with a high-k dielectric layer, Phys. Status Solidi A 211 (2014) 784.
[15] N. Zhang, H. Yokota, A.M. Glazer, Z. Ren, D.A. Keen, D.S. Keeble, P.A. Thomas, Z.-G. Ye, The missing boundary in the phase diagram of $PbZr_{1-x}Ti_xO_3$, Nature Commun. 5 (2014) 5231.
[16] Y.L. Zhu, S.J. Zheng, X.L. Ma, L. Feigl, M. Alexe, D. Hesse, I. Vrejoiu, Microstructural evolution of $[PbZr_xTi_{1-x}O_3/PbZr_yTi_{1-y}O_3]$ n epitaxial multilayers (x/y = 0.2/0.4, 0.4/0.6)–dependence on layer thickness, Philos. Mag. 90 (2010) 1359.
[17] J.C. Agar, A.R. Damodaran, M.B. Okatan, J. Kacher, C. Gammer, R.K. Vasudevan, S. Pandya, L.R. Dedon, R.V.K. Mangalam, G.A. Velarde, S. Jesse, N. Balke, A.M. Minor, S.V. Kalinin, L.W. Martin, Highly mobile ferroelastic domain walls in compositionally graded ferroelectric thin films, Nat. Mater. 15 (2016) 549.
[18] A.R. Zomorrodian, A. Messarwi, N.J. Wu, AES and XPS study of PZT thin film deposition by the laser ablation technique, Ceram. Int. 25 (1999) 137.
[19] J.-G. Ramí rez, A. Cortes, W. Lopera, M.E. Gó mez, P. Prieto, Scaling Laws in PZT Thin Films Grown on Si (001) and Nb-Doped $SrTiO_3$ (001) Substrates, Braz. J. Phys. 36 (2006) 1066.
[20] H.W. Song, The Effect of Deposition Temperature of $Pb(Zr, Ti)_O3$ (PZT) Thin Films with Thicknesses of around 100 nm on the Piezoelectric Response for Nano Storage Applications, World J. Condens. Matter Phys. 2 (2012) 51.
[21] C.L. Sun, J.J. Hsu, S.Y. Chen, A. Chin, Effect of Zr/Ti Ratios on Characterization of $Pb(Zr_xTi_{1-x})O_3$ Thin Films on Al_2O_3 Buffered Si for One-Transistor Memory Applications, J. The Electrochem. Soc. 150 (3) (2003) G187.
[22] J.Y. Jo, S.M. Yang, H.S. Han, D.J. Kim, W.S. Choi, T.W. Noh, Composition-dependent polarization switching behaviors of (111)-preferred polycrystalline Pb $(Zr_xTi_{1-x})O_3$ thin films, Appl. Phys. Lett. 92 (2008) 012917.